

Redox-Triggered Control of Cell Adhesion and Deadhesion on Poly(lysine)- g -poly(ethylene oxide) Adlayers

Louise Hespel, Julien Dupré de Baubigny, Pierre Lalanne, Simon de Beco, Mathieu Coppey, Catherine Villard, Vincent Humblot, Emmanuelle Marie, Christophe Tribet

▶ **To cite this version:**

Louise Hespel, Julien Dupré de Baubigny, Pierre Lalanne, Simon de Beco, Mathieu Coppey, et al.. Redox-Triggered Control of Cell Adhesion and Deadhesion on Poly(lysine)- g -poly(ethylene oxide) Adlayers. ACS Applied Bio Materials, 2019, 2 (10), pp.4367-4376. 10.1021/acsabm.9b00601 . hal-02301433

HAL Id: hal-02301433
https://hal.science/hal-02301433

Submitted on 3 Oct 2022

HAL is a multi-disciplinary open access archive for the deposit and dissemination of scientific research documents, whether they are published or not. The documents may come from teaching and research institutions in France or abroad, or from public or private research centers.

L'archive ouverte pluridisciplinaire **HAL**, est destinée au dépôt et à la diffusion de documents scientifiques de niveau recherche, publiés ou non, émanant des établissements d'enseignement et de recherche français ou étrangers, des laboratoires publics ou privés.

Redox-triggered control of cell adhesion and deadhesion on poly(lysine)-g-poly(ethyleneoxide) adlayers.

Louise Hespel,[1] Julien Dupré de Baubigny,[1] Pierre Lalanne,[1] Simon de Beco,[2] Mathieu Coppey,[2] Catherine Villard,[2] Vincent Humblot,[3] Emmanuelle Marie,[1] Christophe Tribet.[1]*

1 PASTEUR, Département de chimie, École normale supérieure, PSL University, Sorbonne Université, CNRS, 75005 Paris, France

2 Laboratoire Physico Chimie, Institut Curie, PSL Université, Sorbonne Université, CNRS UMR168, F-75005 Paris, France

3 Laboratoire Réactivité de Surface, Sorbonne Université, CNRS UMR 7197, 4 place Jussieu, Paris France

* christophe.tribet@ens.fr

Abstract.

Spontaneous adsorption of poly(lysine)-g-poly(ethyleneglycol) comb-like copolymers (PLL-g-PEG) is a versatile mean to coat substrates with polymer layers that resist cell adhesion. We prepared redox cleavable PLL-g-PEG to switch adhesion on demand. Redox sensitivity was obtained by introducing disulfide linkers between the PLL backbone and PEG strands. This modification was done alone or in combination with an azide-end on the PEG strands that enabled in situ conjugations of adhesion peptides or fluorescent labels (by simple application of commercially available molecules for copper-free click chemistry compatible with cell survival). To balance the functional (adhesion-promoting) vs cell-repellent copolymers, mixed layers of adjusted compositions were obtained by coadsorption from mixed solutions of the cleavable copolymer with non-cleavable and repellant PLL-g-PEG. The deposition of copolymers and quantitative cleavage as triggered by reductive conditions (application of solutions of tris(carboxyethyl)phosphine, dithiothreitol or gluthatione) were characterized by QCM-D, XPS, and fluorescence microscopy. In cell culture conditions, redox-triggered cleavage was obtained by non toxic application of TCEP for a few minutes, enabling either to release cell attachment points (i.e. cleavage of RGD-presenting areas) or to "open" non-specific adherent areas (i.e. transition from PEG-presenting areas to adherent PLL-like coatings).

keywords. redox responsive, dynamic coatings, micropatterns, disulfide, PLL-PEG antifouling, cell adhesion.

Introduction.

Deposition of a soft polymer layer on the top of substrates provides a versatile control on the interface between cells and surface for in vitro cultures. These coatings can either diminish non-specific adhesion (*e.g*. poly(ethyleneglycol), PEG) or facilitate cell binding (poly(lysine), PLL). They are easily micropatterned to guide cell growth or migration, enabling investigation on how cells adapt to complex interfacial constraints.[1] Typical applications include studies of cell-cell communication (*e.g.* neuron networks,[2,3] control of stem cell fate,[4] co-cultures for tissue engineering, etc.[5] Recently, dynamic interfacial layers were introduced in order to modulate cell-surface interaction with temporal control. The typically goal is to switch substrates between a repellent and an adhesive state [6,7,8,9, 10,11]). Changing adhesiveness in a time-controlled manner is key to recapitulate or mimic the spatio-temporal variations occurring in the interactions between cells and the natural extracellular matrix. It has been shown that a single *in situ* on/off switch can affect cell fate (e.g. gene expression pattern depends on the delay of peptide display after cell deposition on a substrate)[12]. Providing a robust *in situ* and on-demand switch between cell-repellency and cell binding is however challenging. Robustness refers here to i) preservation of the interfacial response during cell growth, in cell culture media, ii) providing high contrast between specific *vs* non-specific binding, and iii) the absence of toxicity. To reach this goal it is key to coat the substrates with a dense array of cell-repellent (antifouling) polymer strands such as PEG, in order to minimize both non-specific interactions and adsorption of contaminants (e.g. biomolecules present in culture media). Points ii) and iii) can be fulfilled by bioorthogonal or non-toxic, covalent attachment or detachment of adhesion-controlling chemical moieties. For instance, click chemistries have been reported for mild attachment of adhesion cues (e.g. peptides onto functional PEG strands [13,14,15]). On the other hand, light-triggered cleavages of photo-labile

linkers have been implemented to release either PEG strands or adhesion peptides.[16,17,18,19] UV irradiation is however required to cleave these photocages. Possible toxicity on fragile cell lines, together with interferences with imaging by optical microscopy introduces significant constraints that motivates active researches of new photocages.[20, 21]

Mild variation of the redox potential is an interesting alternative trigger that does not suffer the same constraints as photo-cleavage. A few examples of redox-triggered adhesion/deadhesion of cells are reported: coating with PEDOTs,[22,23,24] use of metalized substrates to trigger desorption or reductive cleavage by variation of surface potential as for instance of thiol-based self-assembled monolayers on gold,[25,26] electrochemical change of the charge of ferrocene in multilayers,[27] swelling of surface-bound host:guest complexes.[28] The examples above are useful for cell harvesting, but they all require macromolecule-decorated electrodes. The need for electron-conductive surfaces and specialized chemistry skills may hamper a broad adoption of such technologies. It is on the other hand possible to rely on changes in redox potential in solution, *e.g.* by injection of reductive agents. In this line, redox sensitive assemblies and capsules used as drug-delivery systems in nanomedicine were designed by introduction of key labile linkers (in particular disulfide bonds).[29,30,31,32] A few reports also suggest their use for on-demand deadhesion.[33]

The implementation of redox-cleavable and biocompatible layers by easy-to-handle and versatile surface chemistries has however not been reported to our knowledge. Of particular importance, adjustment of surface properties must be manageable by end-users, using bench-top facilities available in biology laboratories, and ideally both the attachment and detachment of cells have to be controlled. We propose here a redox control of adlayers made of functionalized

poly(lysine)-g-poly(ethyleneoxide). PLL-g-PEG copolymers were first proposed and developed by Textor et al.[34,35] as one of the more versatile tools to obtain biocompatible and protein-repellent coatings by straightforward adsorption on a large diversity of materials. An adlayer of PLL-g-PEG can achieve antifouling on plastics, ceramics, metal oxydes, etc. Surface protection by PLL-g-PEG is now applied in micropatterning methods for mammal cell cultures [36,37, 38] and is used in commercial biosensors and biomedical microdevices.[39,40,41] We added two functions into PLL-g-PEG derivatives: first, a disulfide linker between the PLL backbone and PEG side chains (PLL-g-SSPEG) made it redox cleavable. Second, introduction of azide-ended PEG strands (PLL-g-SSPEGN_3) enabled copper-free click conjugation with adhesion peptides.[42] We explored different combinations and adjustments of the functional PLL-g-PEG derivatives to switch substrates either from repellency to adhesiveness, or adhesiveness to repellency. The deposition of modified PLL-g-SSPEG was monitored by quartz crystal microbalance (QCM-D) and surface composition was assessed by XPS. Study of cleavage and release of PEG strands in the presence of reducing agents (tris(2-carboxyethyl)phosphine, dithiothreitol, glutathione) was evidenced by QCM-D complemented by epifluorescence. Mixed adlayers of various compositions were obtained by co-adsorption of repellent (PLL-g-PEG) and disulfide-containing copolymers, which was key to optimize interaction with cells. An important outcome of the study is that depending on the layer composition, transient exposure (including in cell culture medium) with a mild reducing agent enables either redox-triggered transitions from a cell-adhesive to a non-adhesive layer, or the reverse transition from non-adhesive toward adhesiveness (Fig. 1).

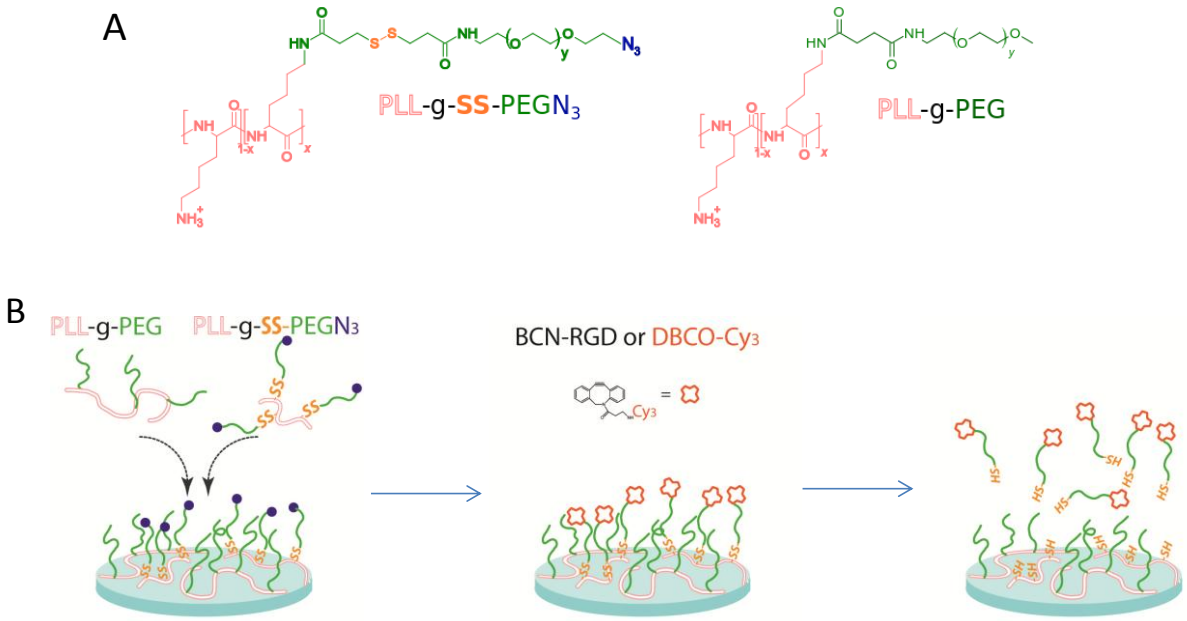


Figure 1. Schematic principle of a redox cleavable coating of PLL-g-PEG comblike copolymer derivatives. A) Structure of the cleavable PLL-g-SSPEGN$_3$ and non-cleavable, cell-repellant, PLL-g-PEG ; B) co-deposition of a mixed adlayer made of redox cleavable, azide-ended, polymers and non-cleavable ones and "click" post-attachment of RGD peptide or a fluorophore; specific release upon redox stimulation of adhesion-promoting strands.

Materials and Methods.

Polymer synthesis. Materials, synthesis and NMR characterizations are provided in supporting information parts 1-5 and Fig. S1-S3). Synthesis was completed in two steps. Briefly, the lysine residue of poly(lysine) (20 000 g/mol) was modified by conjugation with 3-(2-pyridyldithio)propionate (SPDP) to yield a reactive parent chain, PLL-PDP. In the second step, α-thio-poly(ethyleneglycol) (with either a methoxy or an azido end group at ω position) were reacted with the PLL-PDP to obtain comb-like derivatives by disulfide bond formation (Figure S1 in supporting information).

Synthesis of PLL-PDP. PLL (20 kDa, 11.4mg of the hydrobromide form, 1Eq Lysine) was dissolved in 0.5mL sodium tetraborate-HCl buffer (50 mM, pH= 8.4). After complete dissolution, SPDP in 0.3 mL of anhydrous DMSO (5.9 mg, 0.019mmol, 0.33Eq Lysine) was added. The mixture was stirred overnight under inert atmosphere at 35°C. Dialyzis against water for one day (five changes of the bath, Slide-A-Lyzer Thermo Scientific, MWCO 7 kDa) and freeze-drying yielded PLL-PDP as a white powder with a yield of 75%. The percentage of 29 mol% of modified lysine residue was determined by ^{1}H-NMR analysis in D_2O (see supporting data).

^{1}H-NMR (D_2O, 300 MHz): δ (ppm) 8.4 (m, pyridyl, 1H) 7.8 (m, pyridyl 1.9H), 7.25 (m, pyridyl, 1H), 4.3(m, PLL backbone's proton, 3.3H), 3.14-3.0 (m, CH2-SS-pyridyl, α-amide grafted residue, α-amine free residue, 9.1H), 2.65 (m, CH2-CH2-SS-pyridyl, 2.1H), 1.7 (m, aliphatic PLL side chains, 22.2H) (Figure S3)

Synthesis of PLL-g-SSPEG derivatives. PLL-PDP (6.6 mg, 1Eq PDP) was dissolved in 1.5mL of PBS pH 7.4 under inert atmosphere. To obtain the repellent, methoxy-ended derivative, α-thio,ω-OMe-poly(ethylene glycol) (MeO-PEG2000-SH from Sigma-Aldrich, 16.5mg, 1.25Eq PDP) was added. The mixture was stirred overnight under inert atmosphere at room temperature, prior to dialysis against water (Slide-A-Lyzer Thermo Scientific, MWCO 7kDa, five changes of bath). Freeze-drying yielded PLL-g-SSPEG as a white powder. The percentage of 27 mol% PEG-grafted lysine was determined by ^{1}H-NMR analysis in D_2O (see Fig. S3 in supporting information). The final PLL-*g*-SSPEG is recovered by dialyzing against water and then by freeze drying. A similar procedure was used to prepare PLL-*g*-SSPEG (PEG Mw = 5000 g/mol). The percentage of 31 mol% PEG grafted lysine was determined by ^{1}H-NMR analysis in D_2O). To

assure the removal of all residual PDP, cysteamine is added in presence of the grafted polymer in PBS solution.

A similar procedure was used to prepare the azide-ended copolymer by reacting α-thio,ω-azido-poly(ethylene glycol) with PLL-PDP. The azido-ended PEG was synthesized from N_3-PEG-NH_2 (Rapp Polymere, Mw of 3kDa, 50.3 mg). N_3-PEG-NH_2 was dissolved in 5mL of chloroform in presence of trimethylamine (4.3 µL, 2Eq) and stirred overnight under argon atmosphere at room temperature with SPDP (10.6 mg, 2.1Eq). After evaporation of the solvent, the crude was dissolved in 1mL milliQ water for dialysis (cut off 0.5-1kDa) overnight and freeze-dried to yield the PDP-PEGazido polymer. Then the PDP-PEGazido polymer was stirred 3h in a solution of dithiothreitol (from Sigma Aldrich, 20mM) and finally dialyzed (cut off 0.5-1kDa) overnight and freeze-dried to yield the α-thio,ω-azido-poly(ethylene glycol). Yield 92%. The presence of thiol group was confirmed by ^{1}H-NMR (Figure S4). Finally, a similar procedure as for PLL-g-SSPEG was used to prepare PLL-g-SSPEGN_3. The percentage of 28 mol% PEG-grafted lysine was determined by ^{1}H-NMR analysis in D_2O (see supporting data Fig. S4).

PLL-g-SSPEG (ratio of PEG:lysine units of ~1:3) ^{1}H-NMR (D_2O, 300 MHz): δ (ppm) 4.3(m, PLL backbone's proton, 3.7H), 3.7 (m, PEG, ~200H), 3.39 (s, methoxy group, 3H) 3.2 (m, CH2-SS, 2.3H), 3 (m, α-amide grafted residue, α-amine free residue 10.8H), 2.68 (m, CH2-CH2-SS ,2H), 2-1.2 (m, aliphatic PLL side chains, 29.3H) (Figure S3).

PLL-g-SSPEGN_3 (grafting ratio of ~1:4) ^{1}H-NMR (D_2O, 300 MHz): δ (ppm) 4.3 (m, PLL backbone's proton, 2.7H) 3.7(m, PEG, ~200H), 3.2 (m, C**H2** -SS, 2H),3 (m, α-amide grafted residue, α-amine free residue 5.9H), 2.68 (m, C**H2**-CH2-SS, 3H), 2-1.2 (m, aliphatic PLL side chains, 15.5H) (Figure S4).

Synthesis of PLL-g-PEGN$_3$:

The synthesis of azide ended PLL-*g*-PEG has been described in previous studies [15]. Briefly, N-hydrosuccinimide (NHS) was first reacted with glutaryl dichloride to yield to di-NHS-glutaric acid ester. Then, it was added to a solution of α-amino-ω-azido-poly(ethylene glycol)$_{67}$ in CH_2Cl_2 to obtain NHS-activated azido PEG. Finally, NHS-activated azido PEG was finally mixed in a solution of PLL, HBr in a sodium tetraborate buffer (pH=8.5) to yield the *PLL-g-PEGN$_3$*.

QCM-D measurements.

QCM-D analysis were performed using QSense Explorer 401 with a QSense Flow Module 401 from Biolin Scientific. Quartz sensors QSensor QSX 303 SiO2 are also provided by Biolin Scientific and top coated with silicon dioxide. Before measurements the SiO2 quartz sensor was rinsed inside the chamber with NaOH (1M) and SDS (2%v) solution. Then the cell was rinsed continuously with PBS buffer untill signal stabilization at 25°C is reached. Solutions of PLL, PLL-g-PEGN$_3$, and PLL-gSSPEGN$_3$ were prepared in PBS buffer (0.1 g/L). TCEP reducing agent was dissolved in PBS and pH was adjusted at 7.2 with aliquot of 1M NaOH. Solutions were injected at a flow-rate of 0.2 mL/min.

XPS measurements.

XPS analyses were performed using an Omicron Argus spectrometer (Taunusstein, Germany) equipped with a monochromated AlKα radiation source (hν = 1486,6 eV) working at an electron beam power of 300 W. Photoelectrons emission was analyzed at a takeoff angle of 90°; the analyses were carried out under ultra-high vacuum conditions ($\leq 10^{-10}$ Torr) after introduction via

a load-lock into the main chamber. Spectra were obtained by setting up a 100 eV pass energy for the survey spectrum and a pass energy of 20 eV was chosen for the high resolutions regions. Binding energies were calibrated against the C1s binding energy of aliphatic carbon atoms at 284.8 eV. Element peak intensities were corrected by Scofield factors.[43] Casa XPS v.2.3.15 software (Casa Software Ldt, UK) was utilized to fit the spectra and Gaussian/Lorentzian ration was applied (G/L ration = 70/30). *Sample preparation*: silicium wafers were cleaned by i) sonicated in acetone for 10 min, ii) acetone:ethanol 50/50 v/v for 10min and rinsing with Milli-Q water, prior to iii) be plunged for 15 min in pyranha solution, rinsed with Milli-Q water and dried. Just before polymer deposition, wafers were treated for 2h in UV-ozone cleaner and stored in Milli-Q water at 4°C before being transferred into a solution of PLL-*g*-SSPEGN_3 in water (1 mg/mL) for 1 h. Treatment by reducing agent consisted of an 1h incubation in a 5 mM solution of either TCEP or GSH and in a 10 mM solution of DTT. Finally, the samples were rinsed with Milli-Q water and dried.

Epifluorescence imaging of cleavage.

For epifluorescence microscopy, glass coverslips were coated with microstripes of PLL-g-PEG (25µm width) separating stripes of Cy3-conjugated PLL-g-SSPEGN_3 (6 µm). Coating and micropatterning was obtain by i) bath application for 30 min. in 0.1 g/L PLL-PEG of a clean glass coverslip (preconditioning: wash with HPLC grade ethanol, cleaning by N_2 plasma cleaner during 1 min), ii) rinsing with water and drying under a flush of dust-filtered compressed air , iii) UV etching using a chromium quartz photomask (Delta ask, Enschede, The Netherlands/Toppan product types 5" QZ M1X , deep UV light for 15 min) pressed onto a ~2µL drop of water, iv) bath application of 0.1 g/L PLL-g-SSPEGN_3 aqueous solution (20 µL, 30 min.) and final rinsing

with water. Fluorescence labelling was obtained by application for 60 min. of a drop (20µL) of 50 µM DBCO-Cy3 in water, sandwiched between a PARAFILM® and the coverslip. Extensive washing with 150mM NaCl and water was used to remove unbound fluorophore. The final pattern was observed by epifluorescence microscopy (excitation at 525 nm, 1s exposure/image) with coverslips mounted in a flow cell under a constant flow of aqueous solution of the reducing agent.

Cell adhesion on mixed PLL-g-PEG:PLL-g-SSPEG.

Cleaned and preconditioned microscope coverslip (rinsed with HPLC grade ethanol, 15 min sonication in 1M NaOH, and rinsing with milli-Q water) were coated (same conditions as above) by application for 30 min of a mixed solution of PLL-g-SSPEG and PLL-PEG at a total concentration of 1 g/L and varying the weight ratio of the two polymers. Another coating made with a solution of poly(lysine), PLL, was used as a reference for highly adhesive layer. Plates were rinsed with water and dried under dust-filtered compressed air. Half of this set of coated coverslips was DTT-treated (resp. TCEP) by plunging the plates in a solution of 10mM DTT for 10min (resp. 5min for TCEP), then rinsing with water. Redox-treated, or non-treated coverslips were immersed in 24-well plates containing cell culture medium (DMEM high glucose, Sigma, calf serum 10%). 30 000 HeLa cells were seeded on each well, and incubated at 37°C under CO_2 atmosphere. Average numbers of deposited round-like and of spread cells were determined by random picking of 0.16 mm² areas to reach a total number of 100-120 cells.

Cell detachment from mixed PLL-PEG:PLL-g-SSPEGN_3 post-conjugated with RGD.

Cleaned and preconditioned microscope coverslips were coated by application of a mixed solution of PLL-g-SSPEGN_3 : PLL-PEG (total polymer concentration of 1 g/L) as described above. The coverslips were rinsed with water, prior to application for 1 hour of a 100 mM BCN-RGD Synaffix, Netherland) to "click" the adhesion promoting peptide. After extensive water rinse, coverslips were immersed in DMEM high glucose (Sigma), calf serum 10%, and HeLa cells were seeded (30 000 cells per well), incubated at 37°C under CO_2 atmosphere for 4 h. At time 4 h, the medium was gently removed by aspiration, and replaced by fresh DMEM. Random observation of the plates confirmed that cells were predominantly adherent and spread on the coated glass. The wells were supplemented with TCEP stock solution to reach a final TCEP concentration of 2 mM. After 4h of incubation with TCEP, the medium was smoothly aspirated and replaced by fresh DMEM.

Cell escape from disk patterns.

Cleaned and preconditioned coverslips were coated by application of 0.1 g/L solution of PLL-g-SSPEG as described above, rinsed with water and dried. The coverslips wetted with ~2µL water were pressed on a chromium quartz photomask and exposed to deep UV light for 15 min (similar procedure as describe above for fluorescence imaging) to etch microdisk of 35µm of diameter. Bath application of 0.1 g/L mixed solution of PLL-g-SSPEGN_3 : PLL-PEG (5:95 wt/wt) was used to deposit the cleavable copolymer layer on the etched disks. The coverslips were rinsed with water, prior to bath application for 1 hour of a 100 mM BCN-RGD to conjugate the adhesion promoting peptide. To deposit cells, coverslips were immersed in DMEM high glucose (Sigma), without calf serum, and HeLa cells were seeded (200 000 cells per well), incubated at 37°C under CO2 atmosphere. After 30 min., the medium was gently removed by

aspiration, and replaced by fresh DMEM. At time 4h, observation of the plates confirmed that cells were predominantly adherent on patterned disks. Then a solution of TCEP in phosphate buffer was added in the medium to reach a final concentration of 2 mM. After 30 min at 37 °C, the medium was smoothly removed and replaced by fresh DMEM with calf serum 10%.

Results.

Synthesis of comb-like cleavable PLL copolymers.

Seeking for a straightforward preparation of redox-responsive polymer layers, we introduced disulfide bonds into derivatives of comblike poly(ethyleneoxide)-grafted poly(lysine). As established by Textor and colleagues PLL-g-PEG adlayers circumvents to non-specific adhesion onto materials that are commonly used as cell substrates and implants.[36,34] In addition, modifications on the PEG strands with adhesion-promoting peptide mediate specific cell:polymer attachment points. [42],[44, 45] Following this tracks, disulfide linkers were positioned between the PLL backbone and PEG side chains. PEG strands were either methoxy terminated (to obtain antifouling properties) or azide-terminated for copper-free cycloaddition post-conjugation with adhesion peptides (Fig.1). To this end, a parent thiol-reactive PLL chain was prepared by reaction of up to 30 mol% of the amine groups of poly(lysine) (Mw 20 000 g/mol) with succinimidyl 3-(2-pyridyldithio) propionate (see material section and supporting data). The purified thiol-reactive parent chain was reacted in water, either with α-thio,ω-methoxy-poly(ethyleneglycol) (MeOPEG-SH, MW 2000 or 5000 g/mol) to yield the PLL-g-SSPEG, or with α-thio,ω-azido-poly(ethyleneglycol) (N_3PEG-SH, MW 3000 g/mol) to prepare PLL-g-SSPEGN_3 (see experimental section and supporting data). Grafting percentages of respectively, 27 mol%, 31

mol% and 28 mol% PEG-grafted lysine were obtained. A reference, non-cleavable PLL-g-$PEGN_3$ was similarly synthesized.

Cleavage assessment from measurement of adsorbed mass.

Adsorption and reductive cleavage were assessed by quartz crystal microbalance measurements. As a consequence of their cationic backbone, comb-like PLLs adsorb tightly onto anionic surfaces. In PBS buffer of pH 7.2 the deposition of either PLL, or PLL-g-$SSPEGN_3$, or PLL-g-$PEGN_3$, onto plasma cleaned silica-coated quartz started immediately upon flushing polymer solutions (Figure 2). By application of the Sauerbrey model, the apparent (hydrated) masses of deposited layers were estimated at time 10 minutes (when frequency shift reached a plateau) to about 12 mg/m^2 (PLL-g-PEG derivatives) and 7 mg/m^2 (bare PLL). Effective thickness may be calculated from the model, but is in practice highly sensitive to estimates of the specific density of the adlayer. Using common values of 1000 - 1050 g/L, the estimated thickness of all layers were <15 nm, typically of about 1-5 nm for the PLL and of the order of 5 - 15 nm for PEG-grafted PLLs. It is of similar order of magnitude than the diameter of a PEG chain of Mw of 5000 g/mol, and is also comparable to layer thickness of 5-6 nm for PLL-g-PEG as measured by AFM.[46] The layer properties reached a quasi plateau within about one minute (Figure 2B). With PLL-g-SSPEG an additional flushing of either polymer-free buffer or polymer solution did not significantly change the plateau, suggesting that the layer was stable to rinsing (in Fig. 2A). In the case of PLL-g-PEG, a minor additional decrease of the frequency during the second flush of polymer was possibly - but not always- observed and is illustrated in Fig 2A. The magnitude of this second contribution was however always weak if not negligible. It may betray the presence of minor contaminants in some solutions. Eventually, as a control experiment made on non-

cleavable PLL-g-PEGN$_3$ layer (Fig 2A), application of 5 mM TCEP as the reducing agent did not affect the adsorbed mass by more than uncertainty. In contrast, application of reducing agents on PLL-g-SSPEGN$_3$ layers resulted in significant increase of the frequency, i.e. a decrease of the adsorbed mass and release of adsorbed chains (Fig. 2A & B). After a few minutes of exposure to anyone of the reducing agents TCEP, GSH, or DTT, the frequency reached a plateau value that was close to the value measured by deposition of bare PLL, suggesting that most of the PEG chains were released. Differences in the rate of mass release (Fig. 2B) suggested that in PBS at pH 7.0-7.5, the TCEP provides the fastest cleavage (< 3 min.), whereas in the same buffer GSH was almost unable to change significantly the adsorbed mass at time 10 min. Of note in the case of the thiol reducing agents such as DTT and GSH, the thiol-disulfide exchange reaction is reported to primarily proceed via thiolate (having a markedly higher nucleophilicity than thiol) and thus is dramatically affected by pH even far below the thiol pKa.[47] To illustrate that marked acceleration of cleavage can be achieved by increasing the pH, Fig. 2B displays the case of GSH at pH 8.5.

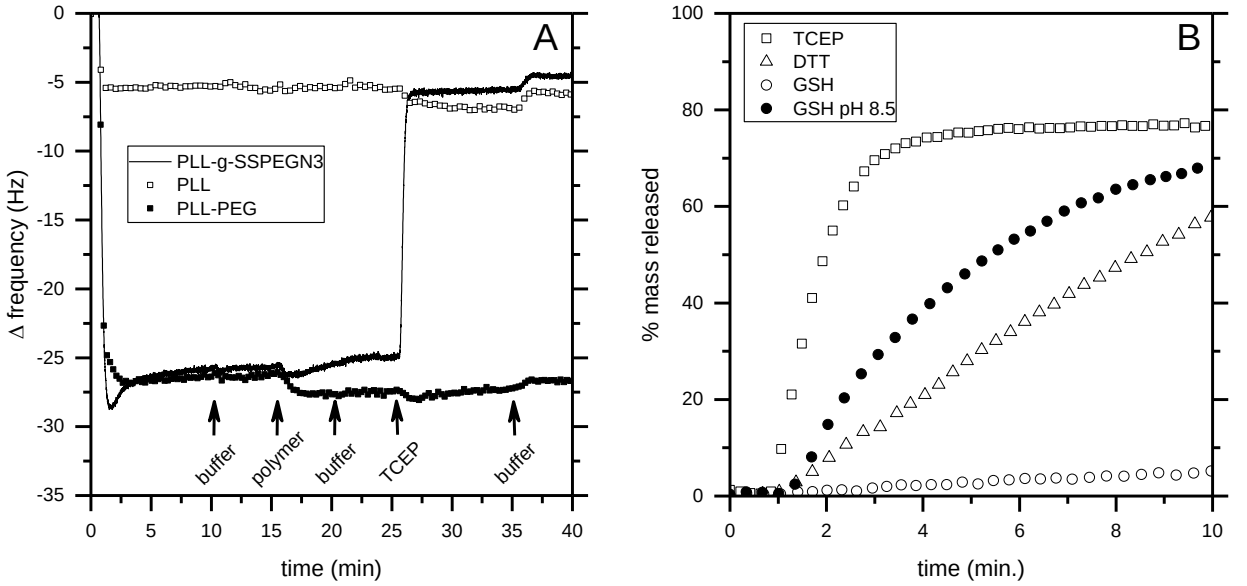


Figure 2. QCM-D characterization of polymer adsorption on silica and exposure to reductive conditions. A) frequency shifts during application of a solution of 0.1 g/L copolymer in 20 mM PBS buffer pH 7.2 (at time zero), followed by rinsing steps including exposure to 5mM TCEP solution in PBS; the complete sequence as quoted by arrows was: polymer in PBS / PBS buffer / polymer in PBS / PBS buffer / TCEP in PBS / PBS buffer. B) Variation of the apparent adsorbed amount of PLL-g-SSPEGN_3 (calculated as % of the frequency variation recovery, with 100% corresponding to bare silica) that was deposited as in fig. 2A and rinsed at time quoted zero with a 5 mM solution of reductive agent (GSH, TCEP, and DTT in PBS buffer with pH adjusted at 7 - 7.5, or pH 8.5 as quoted)

Cleavage assessment from surface chemistry analysis

To assess that treatment with reductive agents specifically detached PEG strands, we performed the analysis of elemental composition of films by X-ray photoelectron spectroscopy (XPS). XPS is probing the thin upper layer (10 nm) deposited on silica wafers (see experimental section). In the C1s spectrum (Fig. 3A), peaks characterizing contributions from carbon atoms can be deconvoluted into three components: one peak at 284.8 eV corresponding to carbon-carbon and carbon-hydrogen contributions (C-C/C-H), one peak at 286.3 eV from ether and amine groups predominantly present in the PEG chains but also in PLL backbone, and a third peak at 288 eV from carbon belonging to amide groups and present in similar amount in the PEG strands and in the PLL backbone. The peak corresponding to ether groups from the PEG strands was markedly diminished upon treatment with reductive solutions of either TCEP, DTT, or GSH (respectively 5, 10 and 5 mM for one hour, Fig. 3). The degree of cleavage was calculated from emission at 286.3 eV due to "non amine" carbons. To this aim, all peaks were normalized by the emission intensity from silica, and contribution from the amine groups of PLL was subtracted (using

emission at 288 eV). The resulting index shown in fig. 3B indicates that before redox cleavage the emission from ether groups is well above background (the background is due to contact with ambient air). It is significantly decreased down to a value similar to background after treatment with TCEP.

Analysis of surface composition was completed by microscopy imaging using fluorescently-labeled PEG strands. To assess PEG cleavage by fluorescence, stripes of PLL-g-SSPEGN_3 (of 6μm width) were patterned on glass coverslips. The PEGazide ends were labeled by click conjugation of DBCO-Cy3 (see experimental section). The stripes of PLL-g-PEG deposited next to the PLL-g-SSPEG-Cy3 ones were used as in situ references of non-fluorescent background (Fig. 4). The coverslips were imaged under a constant flow of a solution of TCEP reducing agents (200 μL/min.). Loss of labeled PEG strands over time was observed as a rapid decrease of the contrast between background and fluorescent stripes that leveled down to background intensity in a few minutes (Fig. 4A&B). It was noticed during the labelling procedure with DBCO-Cy3 that a rinse with milliQ water could not fully wash out the excess of unconjugated fluorophore (in particular, the background PLL-g-PEG stripes displayed a weak fluorescence in these conditions, presumably due to unspecific adsorption of the fluorophore). The use of a rinsing solution of 300mM NaCl succeeded better to remove unreacted Cy3. For that reason, the solution of 5mM TCEP was flushed either in the presence or absence of NaCl (Fig. 4A). The decrease of fluorescence of PLL-g-SSPEG-Cy3 was observed in all conditions, though in salt-free water the kinetics was slower but possibly reflects in part a retention due to interaction of the Cy3 with the surface. Full cleavage of the disulfide bonds and release of most cleavable PEG chains was validated in NaCl-containing buffers, indicating that loss of mass observed by QCM-D can be attributed to the release of PEG chains.

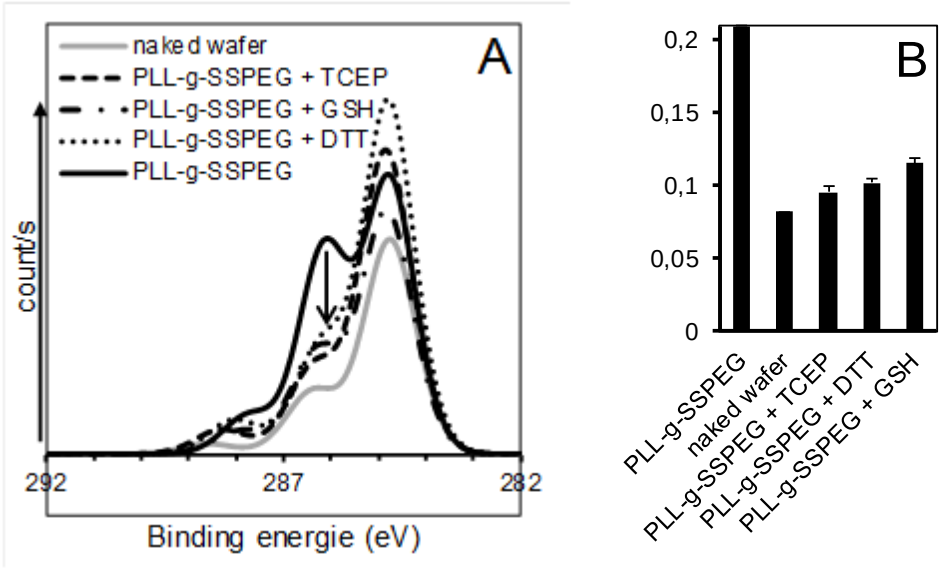


Figure 3. XPS analysis of silica wafer coated with PLL-g-SSPEG. A) spectra before and after 1h incubation in 5 mM solutions of TCEP or GSG and 10 mM of DTT . B) intensity of C-O peak normalized by the contribution of Si from silica.

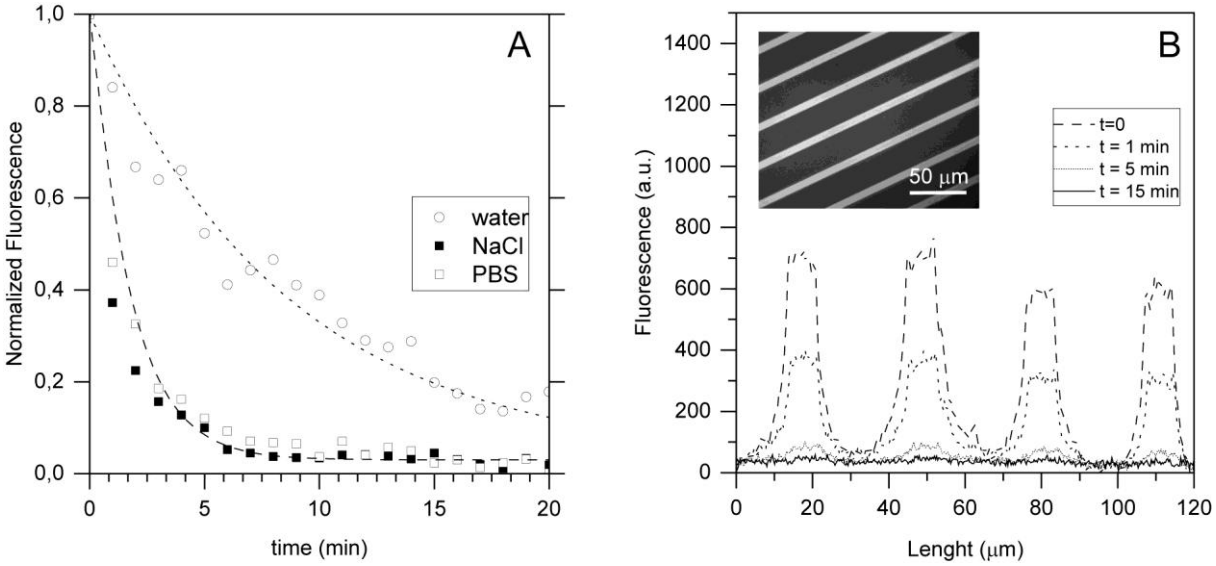


Figure 4. Fluorescence of Cy3-labelled PLL-g-SSPEGN_3 microstripes during exposure to reductive conditions. A) Variation of the average stripe's fluorescence intensity normalized by intensity at time zero during exposure to 5 mM TCEP in either PBS buffer pH 7.2, or milliQ

water with or without 300mM NaCl ; lines are guide for the eye. B) epifluorescence measured along a line orthogonal to the stripes, at increasing time, t, after application of the TCEP solution; a representative fluorescence image at time zero shown in inset.

Cell adhesion on mixed PLL-g-PEG : PLL-g-SSPEG layers

Conditions for using TCEP as a trigger for non-specific cell adhesion were explored. To this aim, we switched the accessibility of the PLL backbone by cleavage of PLL-g-SSPEG. The loss of the PEG protective layer can be used as a non-specific trigger of cell-substrate interactions. In addition, the objective of controlling specific adhesion onto peptide-displaying layers obviously requires that non-specific adhesion can be made negligibly low. In practice, the repellency of layers containing a PLL-g-SSPEG derivative can be modulated by co-deposition of permanently non-adhesive PLL-g-PEG. Increasing fractions of cleavable PLL-g-SSPEG were mixed with PLL-g-PEG to prepare mixed coatings (-SSPEG : -PEG weight ratios of 0:100; 10:90 ; 30:70 ; 50:50 ; 100:0). As a proof of concept, we used HeLa cells, a human cell line that is shared between most laboratories. Adhesion of HeLa cells onto micropatterned substrates has been compared with other cell lines, sp. fibroblasts,[48,49] showing similarities that makes HeLa an interesting generic model to assess basic spreading behavior. Cells were seeded on the homogenous (unpatterned) mixed layers (see experimental section) and the degree of cell spreading was determined by phase contrast microscopy a few hours after seeding (Fig. 5). Cell bodies were predominantly round-like, which indicated that most cells lacked adhesion sites. The surface area of round cells onto PLL-g-PEG, or mixed PLL-g-PEG:PLL-g-SSPEG 90:10 %, or PLL-g-SSPEG 100 % were respectively of 260±40 μm², 420±130 μm² and 310±50 μm². However, on layers prepared with PLL-g-SSPEG above 30 wt%, a fraction as large as 30-40% of

the cells could spread. In addition to change from round to more tortuous shapes, the spread cells showed a higher average surface area of 530 ±180µm² (PLL-gSSPEG 100%). This suggests that PLL-g-SSPEG is not as efficient as the conventional PLL-g-PEG to passivate surfaces (100% PLL-g-PEG is used as reference antifouling systems showing here no spreading, i.e. percentage of spread cells <1% at time 8h, in agreement with the literature [50]). The reason for a poorer repellency of PLL-g-SSPEG is unclear but may rely on a lower degree of grafting of the PLL backbone and/or the use of a slightly shorter PEG (of 3000 g/mol) compared to conventional PLL-g-PEG (of 5000 g/mol). In practice, it was nevertheless possible to obtain adhesion-resistant layers, prior to redox stimulation, by using an excess of PLL-g-PEG chains in mixed coating solutions.

To assess the impact of a reducing agent, cells were seeded on coated coverslips that were pre-exposed to 10 mM TCEP solution for 5 min (see experimental section). In contrast to the observations above, the shape of cells was indicative of a significant adhesion. On mixed layers prepared with more than 30% PLL-g-SSPEG and subjected to redox treatment, the fraction of spread cells at time 8h was above the values of 30-40% observed in the absence of redox treatment, and even above the reference fraction of 65 % that was measured on the fully adhesive PLL layer (Fig. 5B). The contrast between spreading rates before and after redox treatment varied with the % of cleavable -SSPEG strands. Namely, on layers prepared with 10 wt% of PLL-g-SSPEG full adhesion cannot be achieved (spreading of ~30% of the cells, Fig 5B), whereas on layers made with more than 50 wt% PLL-g-SSPEG the maximum of 80-90% spreading was reached. Observation of a higher % of spread cells compared to the reference PLL indicates that redox-treated layers were fully adhesive and allowed for fast rate of spreading. Comparison of the average cell areas confirmed the change of adhesion achieved by redox-triggered cleavage. On

layers made of non-cleavable PLL-g-PEG, the average surface of cells was not significantly affected (260±40µm² without TCEP treatment and 280±90µm² with TCEP treatment). On layers made with 100 wt% of PLL-*g*-SSPEG, the average cells surface markedly increased from 380±150 µm² without TCEP treatment to 720±230 µm² with TCEP treatment (N.B.: as a reference for cell area onto an adhesive substrate, we measured the average cell area on PLL of 500±240 µm²). Here, the average values are calculated on the whole cell population, accounting for both round-like shapes and more elongated ones (which is reflected in the high standard deviation). Accordingly, on substrates having a shallow contrast in adhesiveness, such as substrates prepared at 10 wt% PLL-g-SSPEG, the cell's area was not markedly modified by TCEP treatment (430±130 µm² without TCEP and 380 ±180µm² with TCEP). Another indication of weaker adhesion on substrates predominantly covered by PLL-g-PEG is that adherent cells on the 10 wt% PLL-g-SSPEG layer displayed (after TCEP treatment) a lower area compared to TCEP-treated 100% PLL-g-SSPEG (560 ± 220 µm²), confirming that the tightest adhesion was not reached at low wt% PLL-g-SSPEG. Cleaved PLL-g-SSPEG displays thiol moieties that may play a role in enhanced adhesion as compared to PLL (*e.g.* attachment of serum proteins onto free thiols). Similar trends were observed at incubation time 4h and 24h (Supporting data, Fig. S5 and Fig S6) as well as with DTT as reducing agent (supporting data, Fig. S7 and Fig S8). From the present results we can estimate that densities of cleavable strands should not go above 10 wt% when contributions of non-specific interaction have to be minimized.

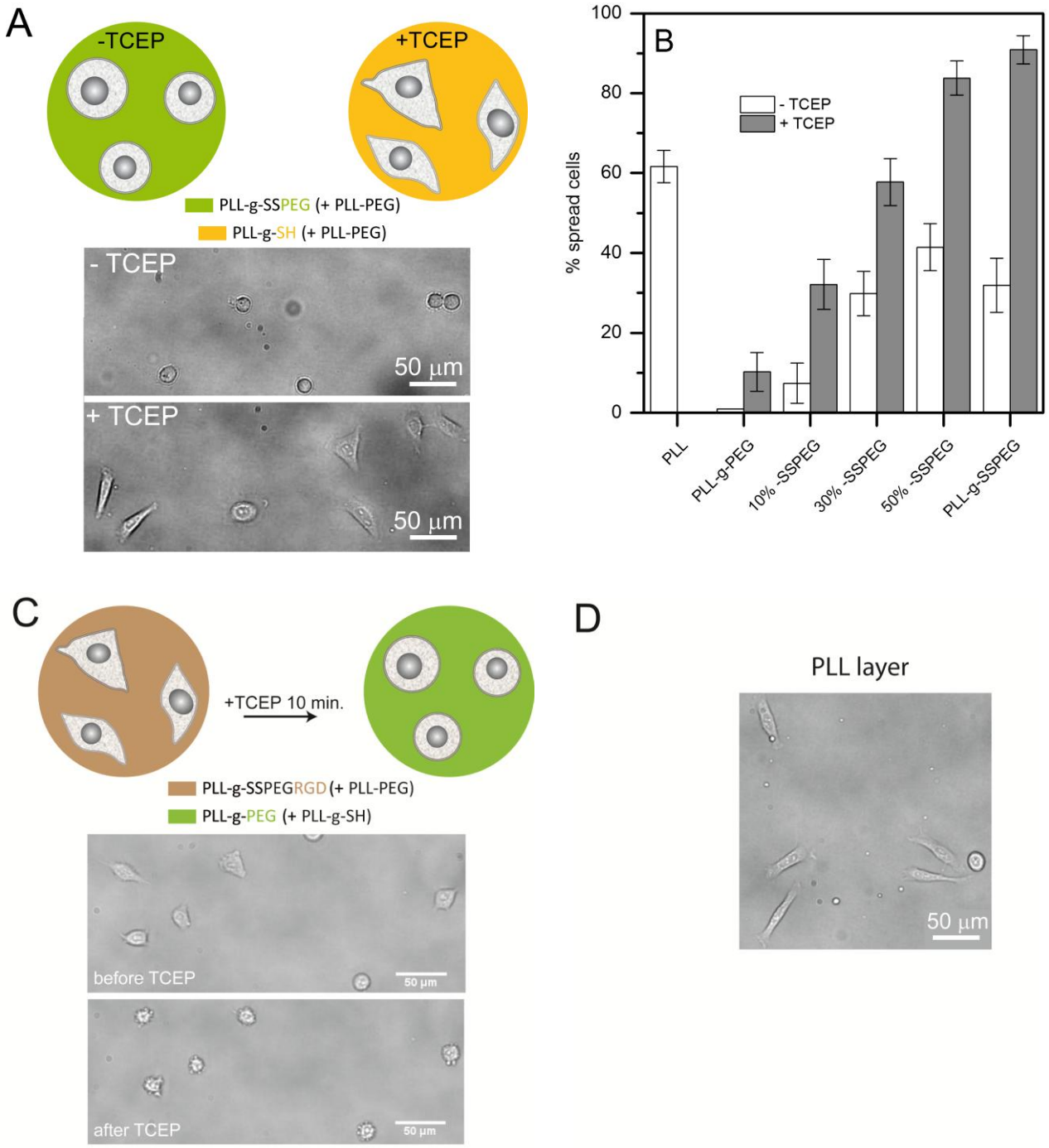


Figure 5. Effect of application of a solution of TCEP on cell adhesiveness. (A) microscopy images and schematic drawing of cells at time 8h deposited onto a 100% PLL-g-SSPEG layer with or without treatment with 10mM TCEP solution prior to cell deposition. (B) % spread cells determined at time 8h onto mixed PLL-g-SSPEG:PLL-g-PEG layers that were (+TCEP) or were

not (-TCEP) pretreated with TCEP. (C) schematic drawing and microscopy images of cells deposited on PLL-g-SSPEGN$_3$:PLL-g-PEG mixed layer (10:90 wt/wt) conjugated with DBCO-RGD prior (top) and after (bottom) supplementation of the culture medium with 5mM TCEP. Cells are shown at time 12 min after introduction of TCEP (5mM), in DMEM, +10% calf serum, 37°C under CO2 atmosphere. (D) HeLa cells at time 8h deposited onto a 100% PLL.

Adhesiveness on RGD-conjugated layers

Cell deposition on peptide-conjugated PLL-g-SSPEGN$_3$ (addition of Arg-Gly-Asp-DBCO) was then considered to mediate specific binding. Accordingly, PLL-g-SSPEGN$_3$ (PEG MW = 3000 g.mol^{-1}) was mixed with >90 wt% PLL-g-PEG to minimize non-specific interactions, and prepare RGD-displaying substrates. A representative example of experiment in Fig. 5 C shows HeLa cells deposited on a layer prepared with 10:90 wt/wt mixed solution of PLL-g-SSPEGN$_3$:PLL-g-PEG (post-conjugated with BCN-RGD, see experimental section). Supplementation with 5mM TCEP in the DMEM culture medium resulted in transition of those cells from spread to round-like shapes within a few minutes, suggesting loss/detachment of the RGD-displaying PEG chains. Of note, when cells were seeded onto a non-cleavable layer of similar composition (i.e. mixed PLL-g-PEGN$_3$: PLL-g-PEG 10:90 wt/wt, post-conjugated with BCN-RGD) their spreading was not affected by exposure to TCEP (Fig. S9 in supporting data). These observations were confirmed by the evolution of the average cell surface. On layers containing cleavable PLL-g-SSPEG-RGD, the average area of cells decreased (from 560±280µm² down to 430±240µm²) whereas it did not change when exposed to TCEP (930±290µm² and 910±260µm² respectively) on layers made of PLL-g-PEG-RGD chains. According to a study by A. Chassepot et. al, application of TCEP is not cytotoxic up to 30 min incubation time (human gingival fibroblasts cells [51]). We checked the

absence of toxicity of TCEP in the present experimental conditions, confirming that HeLa cells were kept alive (see supporting data Fig. S10).

Finally, we illustrate that redox triggering enables cell guidance on micropatterned substrates. We prepared micropatterns made of disk-shaped areas that were UV-etched on a preformed continuous layers of primarily repellant PLL-g-PEG:PLL-g-SSPEG. The etched disks were coated by a PLL-g-PEG:PLL-g-SSPEGN_3 mixed layer, post-functionalized with DBCO-RGD peptide in order to adjust the density of (redox cleavable) adhesive strands. A representative image of HeLa cells seeded onto such patterns is shown in supporting data (Fig. S11), together with example of the absence of impact of TCEP when the disk areas were coated with non-cleavable PLL-g-PEGN_3. Using redox cleavable coating in the disk (here 5 wt% PLL-g-SSPEGN_3, PEG of Mw 5000 shown in Fig. 6), we could similarly confine the cells on the disk area until the redox stimulus is applied. As expected, a short exposure to reductive conditions (2mM TCEP, followed by rinsing with TCEP-free DMEM) rapidly triggered protrusions of cytoplasmic membranes from the cells, followed at hours-long times by spreading and migration of cells toward the outermost regions of the patterns (Fig. 6C).

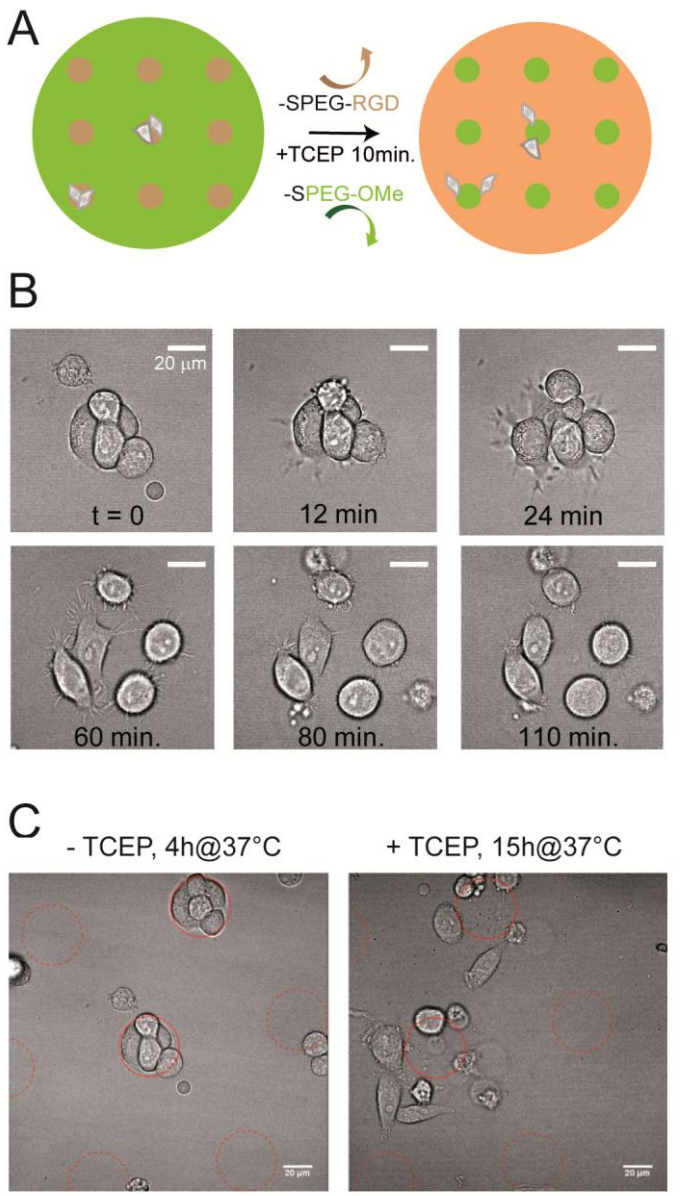


Figure 6. Redox-triggered cell escape from disk micropatterns. (A) schematic drawing of the switch from RGD-presenting microdisks to predominantly repellent, (methoxy-ended) PEG-presenting disks, with concomitant release of the -PEG antifouling strands on the continuous area. (B) time lapse of cells deposited on a disk micropatterned, supplemented at time zero with 2mM TCEP in DMEM ; the medium was replaced by TCEP-free DMEM + calf serum at time 30 min.. Disks were coated by 5 wt% PLL-g-SSPEGN_3 mixed with 95% PLL-g-PEG and the

external continuous area was 100% PLL-g-SSPEG. (C) same as (B) but unzoomed and shown before (left) and 15h after (right) TCPE treatment.

Conclusion.

The present observations indicate that adlayers of PLL-g-SSPEGN_3 enable attachment on surfaces (by copper-free click chemistry) and redox-triggered release of functional groups such as a fluorescent probes or adhesion peptides. When this copolymer is deposited as a mixed layer with non-cleavable PLL-g-PEG, it provides a versatile platform to control the surface density of functional groups. Surface characterizations suggest that a complete cleavage of the disulfide linkers can be achieved within a few minutes. This clean, *in situ* release of an adjustable fraction of (possibly functionalized) PEG chains is obtained via a straightforward procedure and robust surface chemistry that only requires basic benchtop equipments, and uses chemicals that are either commercially available or synthesized in two steps.

When implemented on complex areas, such as micropatterned surfaces, a switch of the presentation (or release) of peptides may roughly mimic signaling and/or gradients of guidance cue in the extracellular matrix. The present redox tools bring the possibility to achieve mild switches both away and below cell bodies. Somewhat arbitrarily and as a proof of feasibility, we showed the deadhesion from disk micropatterns and concomitant adhesiveness of distant areas. Our aim was to illustrate that cell can be guided by tools that avoid requirement for specialized skills or technologies (such as pre-patterned microelectrodes, or copolymer synthesis on surface by "grafting-from" methods), providing rooms for initiatives and optimizations by non-chemists (e.g. adjustment of the surface composition to different culture conditions and cell lines). In addition, PLL has already been adopted as an efficient adhesion-promoting coating on various

cell substrates. This tool can be useful to cell biologists in several contexts including: to study how triggered deadhesion affects cell survival (i.e. anoikis, which is a proposed mechanism for preventing cell growth in "inappropriate" places during embryogenesis), or to trigger differentiation of stem cells and on demand expression of specific genes, , or to induce cell growth or cell retraction on selected surfaces (e.g. to prepare and/or study cell networks, to remodel or establish connections, e.g. between neurons, by opening adhesive paths and removing other areas).

Acknowledgements

This work was supported in part by a grant to C. V and C.T. from IdEx PSL ("switchneurotrail , programme Biologie Mésoscopique), by ANR (CASCADE N° 17-CE09-0019-01to E.M. and C.T.) and "programme investissement d'avenir" ANR-11-LABX-0011.

Supporting Information available: Description of the synthesis and NMR characterization of the polymers, additional data on cell spreading, viability test, illustration of microdisk patterns.

References.

1. Thery, M., Micropatterning as a tool to decipher cell morphogenesis and functions. *Journal of Cell Science* **2010,** *123* (24), 4201-4213.
2. Fricke, R.; Zentis, P. D.; Rajappa, L. T.; Hofmann, B.; Banzet, M.; Offenhausser, A.; Meffert, S. H., Axon guidance of rat cortical neurons by microcontact printed gradients. *Biomaterials* **2011,** *32* (8), 2070-2076.
3. Roth, S.; Bugnicourt, G.; Bisbal, M.; Gory-Fauré, S.; Brocard, J.; Villard, C., Neuronal Architectures with Axo-dendritic Polarity above Silicon Nanowires. *Small* **2012,** *8* (5), 671-675.
4. Phillips, J. E.; Petrie, T. A.; Creighton, F. P.; Garcia, A. J., Human mesenchymal stem cell differentiation on self-assembled monolayers presenting different surface chemistries. *Acta Biomaterialia* **2010,** *6* (1), 12-20.
5. Goubko, C. A.; Cao, X. D., Patterning multiple cell types in co-cultures: A review. *Materials Science & Engineering C-Materials for Biological Applications* **2009,** *29* (6), 1855-1868.

6. Li, W.; Yan, Z. Q.; Ren, J. S.; Qu, X. G., Manipulating cell fate: dynamic control of cell behaviors on functional platforms. *Chemical Society Reviews* **2018,** *47* (23), 8639-8684.
7. Mendes, P. M., Stimuli-responsive surfaces for bio-applications. *Chemical Society Reviews* **2008,** *37* (11), 2512-2529.
8. Yeung, C. L.; Iqbal, P.; Allan, M.; Lashkor, M.; Preece, J. A.; Mendes, P. M., Tuning Specific Biomolecular Interactions Using Electro-Switchable Oligopeptide Surfaces. *Advanced Functional Materials* **2010,** *20* (16), 2657-2663.
9. Dalier, F.; Dubacheva, G. V.; Coniel, M.; Zanchi, D.; Galtayries, A.; Piel, M.; Marie, E.; Tribet, C., Mixed Copolymer Adlayers Allowing Reversible Thermal Control of Single Cell Aspect Ratio. *Acs Applied Materials & Interfaces* **2018,** *10* (3), 2253-2258.
10. Izuta, S.; Yamaguchi, S.; Kosaka, T.; Okamoto, A., Reversible and Photoresponsive Immobilization of Nonadherent Cells by Spiropyran-Conjugated PEG-Lipids. *ACS Applied Bio Materials* **2019,** *2* (1), 33-38.
11. Ren, T. C.; Ni, Y. L.; Du, W.; Yu, S.; Mao, Z. W.; Gao, C. Y., Dual Responsive Surfaces Based on Host-Guest Interaction for Dynamic Mediation of Cell-Substrate Interaction and Cell Migration. *Advanced Materials Interfaces* **2017,** *4* (1), 1500865.
12. Lee, E. J.; Luo, W.; Chan, E. W. L.; Yousaf, M. N., A Molecular Smart Surface for Spatio-Temporal Studies of Cell Mobility. *Plos One* **2015,** *10* (6).
13. Arnold, R. M.; Patton, D. L.; Popik, V. V.; Locklin, J., A Dynamic Duo: Pairing Click Chemistry and Postpolymerization Modification To Design Complex Surfaces. *Accounts of Chemical Research* **2014,** *47* (10), 2999-3008.
14. Gandavarapu, N. R.; Azagarsamy, M. A.; Anseth, K. S., Photo-Click Living Strategy for Controlled, Reversible Exchange of Biochemical Ligands. *Advanced Materials* **2014,** *26* (16), 2521-2526.
15. van Dongen, S. F. M.; Janvore, J.; van Berkel, S. S.; Marie, E.; Piel, M.; Tribet, C., Reactive protein-repellent surfaces for the straightforward attachment of small molecules up to whole cells. *Chemical Science* **2012,** *3* (10), 3000-3006.
16. Abdellatef, S. A.; Nakanishi, J., Photoactivatable substrates for systematic study of the impact of an extracellular matrix ligand on appearance of leader cells in collective cell migration. *Biomaterials* **2018,** *169*, 72-84.
17. Jang, K.; Sato, K.; Mawatari, K.; Konno, T.; Ishihara, K.; Kitamori, T., Surface modification by 2-methacryloyloxyethyl phosphorylcholine coupled to a photolabile linker for cell micropatterning. *Biomaterials* **2009,** *30* (7), 1413-1420.
18. Wirkner, M.; Alonso, J. M.; Maus, V.; Salierno, M.; Lee, T. T.; Garcia, A. J.; del Campo, A., Triggered Cell Release from Materials Using Bioadhesive Photocleavable Linkers. *Advanced Materials* **2011,** *23* (34), 3907-3910.
19. Zheng, Y. J.; Farrukh, A.; del Campo, A., Optoregulated Biointerfaces to Trigger Cellular Responses. *Langmuir* **2018,** *34* (48), 14459-14471.
20. Peterson, J. A.; Wijesooriya, C.; Gehrmann, E. J.; Mahoney, K. M.; Goswami, P. P.; Albright, T. R.; Syed, A.; Dutton, A. S.; Smith, E. A.; Winter, A. H., Family of BODIPY Photocages Cleaved by Single Photons of Visible/ Near-Infrared Light. *Journal of the American Chemical Society* **2018,** *140* (23), 7343-7346.
21. Motta-Mena, L. B.; Reade, A.; Mallory, M. J.; Glantz, S.; Weiner, O. D.; Lynch, K. W.; Gardner, K. H., An optogenetic gene expression system with rapid activation and deactivation kinetics. *Nature Chemical Biology* **2014,** *10* (3), 196-202.
22. Marzocchi, M.; Gualandi, I.; Calienni, M.; Zironi, I.; Scavetta, E.; Castellani, G.; Fraboni, B., Physical and Electrochemical Properties of PEDOT:PSS as a Tool for Controlling Cell Growth. *Acs Applied Materials & Interfaces* **2015,** *7* (32), 17993-18003.

23. Persson, K. M.; Karlsson, R.; Svennersten, K.; Loffler, S.; Jager, E. W. H.; Richter-Dahlfors, A.; Konradsson, P.; Berggren, M., Electronic Control of Cell Detachment Using a Self-Doped Conducting Polymer. *Advanced Materials* **2011,** *23* (38), 4403-4408.
24. Svennersten, K.; Bolin, M. H.; Jager, E. W. H.; Berggren, M.; Richter-Dahlfors, A., Electrochemical modulation of epithelia formation using conducting polymers. *Biomaterials* **2009,** *30* (31), 6257-6264.
25. Yoon, S. H.; Mofrad, M. R. K., Cell adhesion and detachment on gold surfaces modified with a thiol-functionalized RGD peptide. *Biomaterials* **2011,** *32* (30), 7286-7296.
26. You, J.; Heo, J. S.; Kim, J.; Park, T.; Kim, B.; Kim, H. S.; Choi, Y.; Kim, H. O.; Kim, E., Noninvasive Photodetachment of Stem Cells on Tunable Conductive Polymer Nano Thin Films: Selective Harvesting and Preserved Differentiation Capacity. *Acs Nano* **2013,** *7* (5), 4119-4128.
27. Sun, Y.-x.; Ren, K.-f.; Wan, J.-l.; Chang, G.-x.; Ji, J., Electrochemically Controlled Stiffness of Multilayers for Manipulation of Cell Adhesion. *Acs Applied Materials & Interfaces* **2013,** *5* (11), 4597-4602.
28. Gao, T.; Li, L. D.; Wang, B.; Zhi, J.; Xiang, Y.; Li, G. X., Dynamic Electrochemical Control of Cell Capture-and-Release Based on Redox-Controlled Host-Guest Interactions. *Analytical Chemistry* **2016,** *88* (20), 9996-10001.
29. Lee, M. H.; Sessler, J. L.; Kim, J. S., Disulfide-Based Multifunctional Conjugates for Targeted Theranostic Drug Delivery. *Accounts of Chemical Research* **2015,** *48* (11), 2935-2946.
30. Brulisauer, L.; Gauthier, M. A.; Leroux, J. C., Disulfide-containing parenteral delivery systems and their redox-biological fate. *Journal of Controlled Release* **2014,** *195*, 147-154.
31. Su, T.; Cheng, F.; Lin, S.; Xiao, T.; Zhu, Y.; Cao, J.; He, B., Reduction-Induced Decomposition and Self-Aggregation Strategy To Induce Reactive Oxygen Species Generation for Cancer Therapy. *ACS Applied Bio Materials* **2018,** *1* (4), 954-960.
32. Ji, X.; Zhang, R.; Wang, Z.; Niu, S.; Ding, C., Locked Nucleic Acid Nanomicelle with Cell-Penetrating Peptides for Glutathione-Triggered Drug Release and Cell Fluorescence Imaging. *ACS Applied Bio Materials* **2019,** *2* (1), 370-377.
33. Guan, Z. Y.; Wu, C. Y.; Chen, H. Y., Stepwise and Programmable Cell Differentiation Pathways of Controlled Functional Biointerfaces. *Acs Biomaterials Science & Engineering* **2017,** *3* (8), 1815-1821.
34. H.-P.Huang; Michel, R.; Vörös, J.; Textor, M.; Hofer, R.; Rossi, A.; Elbert, D. L.; HubbellSpencer, J. A., Poly(L-lysine)-g-poly(ethylene glycol) layers on metal oxide surfaces: surface-analytical characterization and resistance to serum and fibrinogen adsorption. *Langmuir* **2001,** *17*, 489-498.
35. Ogaki, R.; Foss, M., Biofunctional Surface Patterns Retaining Activity after Exposure to Whole Blood. *Langmuir* **2014,** *30* (23), 7014-7023.
36. Michel, R.; Lussi, J. W.; Csucs, G.; Reviakine, I.; Danuser, G.; Ketterer, B.; Hubbell, J. A.; Textor, M.; Spencer, N. D., Selective molecular assembly patterning: A new approach to micro- and nanochemical patterning of surfaces for biological applications. *Langmuir* **2002,** *18* (8), 3281-3287.
37. Azioune, A.; Storch, M.; Bornens, M.; Thery, M.; Piel, M., Simple and rapid process for single cell micro-patterning. *Lab on a Chip* **2009,** *9* (11), 1640-1642.
38. Strale, P. O.; Azioune, A.; Bugnicourt, G.; Lecomte, Y.; Chahid, M.; Studer, V., Multiprotein Printing by Light-Induced Molecular Adsorption. *Advanced Materials* **2016,** *28* (10), 2024-2029.
39. Strale, P. O.; Bonnemay, L.; Ziane, N.; Opitz, M.; Ruaudel, J., Maskless Quantitative Multi-protein Photopatterning to Orchestrate Cellular Microenvironment. *Biophysical Journal* **2018,** *114* (3), 175A-175A.
40. Wang, J.; Pei, W. H.; Yuan, B.; Guo, K.; Sun, K.; Sun, H. B.; Chen, H. D., An integrated device for patterning cells and selectively detaching. *Biomedical Microdevices* **2012,** *14* (3), 471-481.

41. Czondor, K.; Garcia, M.; Argento, A.; Constals, A.; Breillat, C.; Tessier, B.; Thoumine, O., Micropatterned substrates coated with neuronal adhesion molecules for high-content study of synapse formation. *Nature Communications* **2013,** *4*.
42. van Dongen, S. F. M.; Maiuri, P.; Marie, E.; Tribet, C.; Piel, M., Triggering Cell Adhesion, Migration or Shape Change with a Dynamic Surface Coating. *Advanced Materials* **2013,** *25* (12), 1687-1691.
43. Scofield, J. H., Hartree-Slater Subshell Photoionization Cross-Sections at 1254 and 1487ev. *J. Elec. Spectrosc. Relat. Phenom.* **1976,** *8*, 129–137.
44. Thid, D.; Bally, M.; Holm, K.; Chessari, S.; Tosatti, S.; Textor, M.; Gold, J., Issues of ligand accessibility and mobility in initial cell attachment. *Langmuir* **2007,** *23* (23), 11693-11704.
45. de Beco, S.; Vaidžiulytė, K.; Manzi, J.; Dalier, F.; di Federico, F.; Cornilleau, G.; Dahan, M.; Coppey, M., Optogenetic dissection of Rac1 and Cdc42 gradient shaping. *Nature Comm.* **2018,** *9* (1), 4816-4828.
46. Dalier, F.; Eghiaian, F.; Scheuring, S.; Marie, E.; Tribet, C., Temperature-Switchable Control of Ligand Display on Adlayers of Mixed Poly(lysine)-g-(PEO) and Poly(lysine)-g-(ligand-modified poly-N-isopropylacrylamide). *Biomacromolecules* **2016,** *17* (5), 1727-1736.
47. Nagy, P., Kinetics and Mechanisms of Thiol-Disulfide Exchange Covering Direct Substitution and Thiol Oxidation-Mediated Pathways. *Antioxidants & Redox Signaling* **2013,** *18* (13), 1623-1641.
48. Xia, Y.; Tang, Y.; Wu, H.; Zhang, J.; Li, Z.; Pan, F.; Wang, S.; Wang, X.; Xu, H.; Lu, J. R., Fabrication of Patterned Thermoresponsive Microgel Strips on Cell-Adherent Background and Their Application for Cell Sheet Recovery. *ACS Applied Materials & Interfaces* **2017,** *9* (2), 1255-1262.
49. Yao, X.; Liu, R.; Liang, X.; Ding, J., Critical Areas of Proliferation of Single Cells on Micropatterned Surfaces and Corresponding Cell Type Dependence. *ACS Applied Materials & Interfaces* **2019,** *11* (17), 15366-15380.
50. VandeVondele, S.; Voros, J.; Hubbell, J. A., RGD-Grafted poly-l-lysine-graft-(polyethylene glycol) copolymers block non-specific protein adsorption while promoting cell adhesion. *Biotechnology and Bioengineering* **2003,** *82* (7), 784-790.
51. Chassepot, A.; Gao, L. C.; Nguyen, I.; Dochter, A.; Fioretti, F.; Menu, P.; Kerdjoudj, H.; Baehr, C.; Schaaf, P.; Voegel, J. C.; Boulmedais, F.; Frisch, B.; Ogiert, J., Chemically Detachable Polyelectrolyte Multilayer Platform for Cell Sheet Engineering. *Chemistry of Materials* **2012,** *24* (5), 930-937.

For Table of Content only , TOC graphic

